

# Programming the Sequential Release of DNA

## Supplemental Information

Dominic Scalise<sup>†</sup>, Moshe Rubanov<sup>†</sup>, Katherine Miller<sup>†</sup>, Leo Potter<sup>†</sup>, Madeline Noble<sup>†</sup> & Rebecca Schulman<sup>†‡\*</sup>

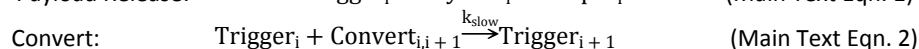
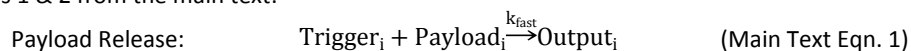
<sup>†</sup>Chemical & Biomolecular Engineering, & <sup>‡</sup>Computer Science, Johns Hopkins University, Baltimore, MD 21218 United States

### SI1: Models and Analysis of the Sequential Release Cascade

Here we use models to explore the kinetics of the sequential release circuit. The first model is a mass-action kinetics model of strand displacement reactions involved in the sequential release process where the reactions are modeled as bimolecular interactions. The second model is also a mass-action kinetic model, but uses the more detailed “three step model” described in reference SI-R1 to model each reaction. Finally, we include additional effects into this three step model, which were not incorporated into the previous two models, including toehold occlusion and the fact that the species as synthesized and assembled are an impure mixture of the desired species and other inert complexes or those able to participate in undesired side reactions. The code that implements each of these models is provided at the end of this section.

#### SI1.1 Ideal Bimolecular Predictions.

The ideal bimolecular unlocked sequential release circuit consists of the abstract chemical reactions in equations 1 & 2 from the main text:



Using  $k_{\text{fast}} = 4 \mu\text{M}^{-1}\text{s}^{-1}$  and  $k_{\text{slow}} = 2 \cdot 10^{-2} \mu\text{M}^{-1}\text{s}^{-1}$ , respectively the approximate reaction rate constants for 7 and 4 nucleotide toehold strand displacement reactions from reference SI-R1, and the same initial reactant concentrations as used in the experiments in the main text (25 nM Payloads,  $37.5 \cdot (4 - i)$  nM  $\text{Convert}_{i,i+1}$  for  $i=1$  to 4, and 112.5 nM of the  $\text{Trigger}_1$ ), we obtain the simulation results in Fig. SI1.1. We observed qualitatively similar behavior to the unlocked sequential release circuit in the experiments presented in Figure 3b, albeit this ideal model predicts roughly 2x faster kinetics of release.

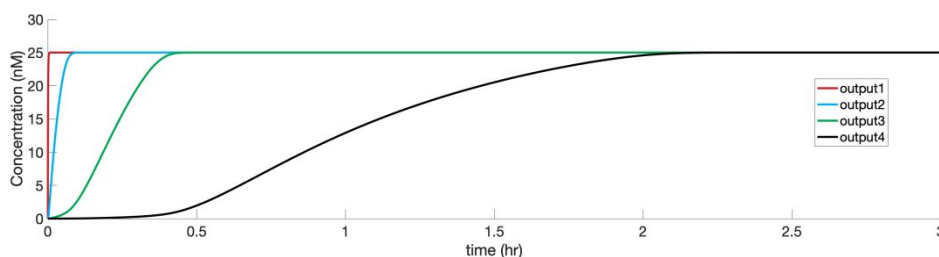


Figure SI1.1 Kinetics of release predicted by the bimolecular model of the unlocked sequential release circuit following Main Text reactions Equations 1 and 2.

We can use the same model to simulate the clocked version of the sequential release circuit, setting the initial concentration of  $\text{Trigger}_1$  to zero and including the mass-conserving version of the clock reaction from the main text equation 5:



We will use  $k_{\text{ont}} = 2 \cdot 10^{-6} \mu\text{M}^{-1}\text{s}^{-1}$ , the approximate reaction rate constant for a 0 nucleotide toehold reaction<sup>SI-R1</sup>, and  $1 \mu\text{M}$  initial concentrations of both Source and Initiator. Running this simulation, we obtain the results in Fig. SI1.2. We observed that the release stages are sharply separated, with a minor slowdown in release timing as stages increase, due to the gradual depletion of Source and Initiator. While this model

matches our design objectives, the stages are substantially more discrete than observed in the experiments in the main text.

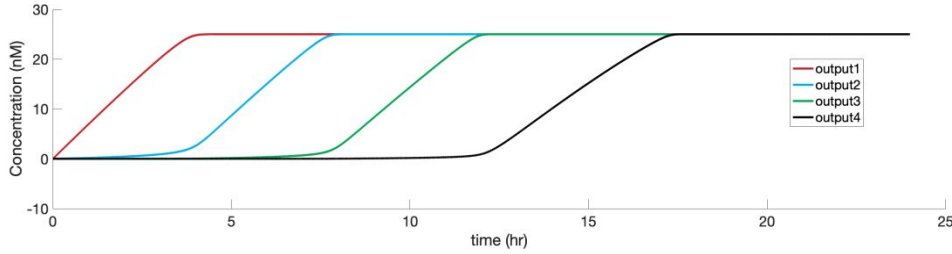
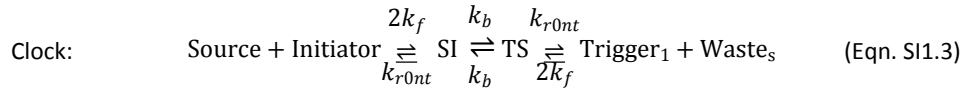
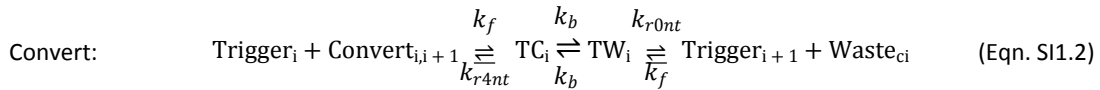
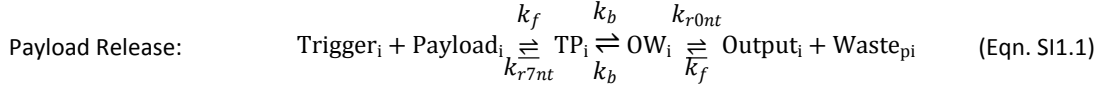


Figure S11.2: Kinetics of release predicted by a model using the bimolecular reactions for clocked sequential release circuit from Main Text Equations 1, 2, and 5.

### S11.2 Predictions of a Three Step Model for the Sequential Release Cascade

The Three Step Model<sup>SI-R1</sup> is a more detailed model of DNA Strand Displacement (DSD) reactions, in which each of the bimolecular reactions from the previous model are split into three reversible steps: (i) the toeholds on the two reactants bind, (ii) the complex undergoes branch migration, (iii) the product toeholds dissociate. With this model, the reactions become:



We used the constant  $k_f = 3.5 \mu\text{M}^{-1}\text{s}^{-1}$  as the association rate constant of DNA hybridization<sup>SI-R1</sup>. We use the constant  $k_b = 400/x^2 \text{ s}^{-1} = 0.907 \text{ s}^{-1}$  as the branch migration rate constant for a branch migration domain of length  $x=21$  nucleotides<sup>SI-R1</sup>. We used the constant  $k_{rYnt} = k_f \cdot 10^6 \cdot (2/x) \cdot e^{(\Delta G^0(Y)/(RT))} \text{ s}^{-1}$  as the toehold dissociation rate constant for a toehold of length  $Y$  nucleotides next to a branch migration domain of length  $x$  nucleotides, where  $\Delta G^0(Y)$  is the standard free energy of the toehold of length  $Y$  nucleotides,  $R = 1.987 \cdot 10^{-3} \text{ kcal}/(\text{mol} \cdot \text{K})$ , and  $T = 298 \text{ K}$ <sup>SI-R1</sup>. We used  $\Delta G^0(7nt) = -9.2 \text{ kcal}/\text{mol}$ ,  $\Delta G^0(4nt) = -4.7 \text{ kcal}/\text{mol}$ , and  $\Delta G^0(0nt) = 1.9 \text{ kcal}/\text{mol}$  for toeholds of length 7, 4 and 0 nucleotides respectively<sup>SI-R1</sup>. We used  $2k_f$  as the toehold association rate for the clock reaction because the Initiator can bind to either side of the Source complex, and similarly used  $2k_f$  for the reverse toehold association rate of the  $\text{Trigger}_1$  and  $\text{Waste}_s$  molecules. Using the same initial concentrations as in the previous bimolecular models (25 nM Payloads,  $37.5 \cdot (4 - i) \text{ nM}$   $\text{Convert}_{i,i+1}$  for  $i=1$  to 4; for the unlocked circuit 112.5 nM of the  $\text{Trigger}_1$  and for the clocked circuit  $1 \mu\text{M}$  each of Source and Initiator), we obtain the unlocked simulation results presented in Fig. S11.3 and the clocked results in Fig. S11.4. The results are qualitatively similar to the bimolecular model. However, the unlocked three step model circuit is now operating about twenty minutes slower than in the bimolecular case, and is approximately a factor of 4x slower than the empirical data in the main text Figure 3b. The clocked three step model circuit is approximately 2x slower than both the bimolecular clocked circuit and the empirical data in main text figure 4c. Compared to the bimolecular model, this initial three-step model did a worse job of capturing the kinetics of sequential release observed in experiments, but better captured the overlapping triggering of stages, where stages begin to trigger before the previous stage has fully released all of the outputs. We thus sought to consider two other effects combined with the three step model, toehold occlusion and the presence of strands or complexes with defects, to better understand how the kinetics that we observed arise and to understand how kinetics can be tuned, while preserving the non-discrete triggering of stages.

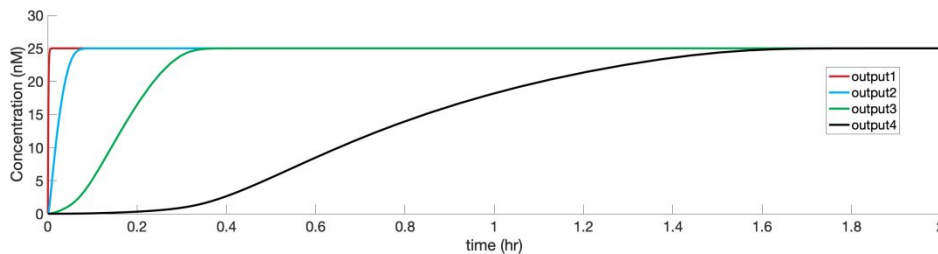


Figure S11.3: Three Step Model simulation of the unclocked sequential release circuit. The reactions, rate constants and concentrations of species are described in SI Section 1.2.

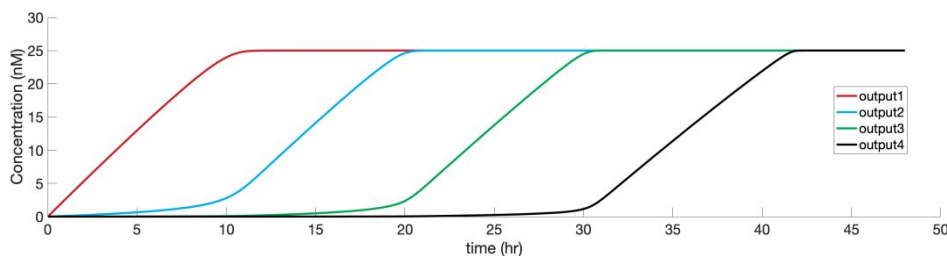
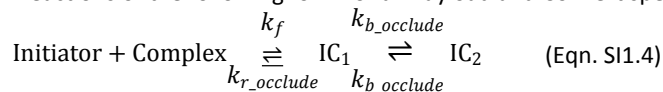


Figure S11.4: Simulated kinetics of the clocked sequential release circuit using the Three Step Model simulation (SI Equations XXX) of the clocked sequential release circuit. The rate constants and concentrations of species are described in SI Section 1.2.

### S11.3 Models to Help Understand the Effects of Toehold Occlusion and Reactant Impurities on the Operation of the Sequential Release Cascade

Using the Three Step Model, we can also simulate the effects of two well known non-idealities found in all DSD reactions, (i) toehold occlusion, and (ii) small fractions of impure reactant populations due to random synthesis errors. In toehold occlusion<sup>SI-R2</sup>, an invading strand can transiently bind to and occupy the complementary toehold of a complex, even if the adjacent branch migration domain is not complementary. Binding of the invading strand temporarily blocks the toehold. While the toehold is blocked, DSD reactions with a correct invader strand cannot be initiated at the toehold. Toehold occlusion can thus slow down reactions involving a toehold that can be occluded in this way. The effects of toehold occlusion are typically exacerbated by high reactant concentrations because an occluding species remains bound to a long toehold for a long time and occluding species bind more often when their concentrations are higher. In the clocked sequential release circuit, the Initiator strand is at a relatively high concentration. While the Initiator cannot complete a full DSD reaction with the Payload or Convert species, it does share a complimentary toehold with all of the payload and convert species, as well as a partial branch migration domain. We can model the effects of toehold occlusion by including the partial DSD reactions of the following form for all Payload and Convert species in our system:



We next include the reactions from Equation S11.4, following the three step model equations in reference SI-R1. These models used a toehold binding energy of  $k_{r\_occlude} = -6.9$  kcal/mol for occlusion between the initiator and each of the payloads and  $-4.7$  kcal/mol between the initiator and each of the convert species with  $k_{r\_occlude} = k_f \cdot 10^6 \cdot (2/21) \cdot e^{(\Delta G^0(Y)/(RT))} s^{-1}$ . This model also used  $k_{b\_occlude} = \frac{400}{9^2} s^{-1}$  for the partial branch migration step of both the payload and convert species in the first stage with  $k_{b\_occlude} = \frac{400}{2^2} s^{-1}$  for the partial branch migration steps for all of the subsequent stages. With these additions to the model, we now observe substantially that the output of downstream stages begins to be released before all of the outputs from the upstream stages are fully released (Fig S11.5) so that the time scales of release better match the time scales of release observed in experiment (Main text Fig. 4c). The toehold occlusion reactions that do not involve the Initiator involve reactants at substantially lower concentrations and are therefore less likely to significantly

impact the kinetics of Sequential Release cascades.

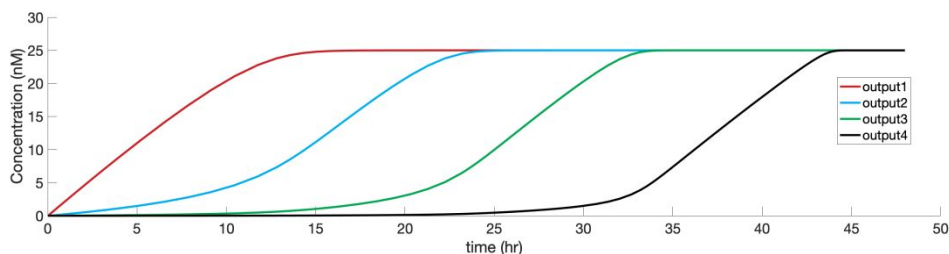


Figure S11.5: Simulated kinetics of the clocked sequential release circuit using the Three Step Model of strand displacement (Equations S11.1-S11.3) incorporating toehold occlusion reactions involving the Initiator strand (Equation S11.4). The Three Step Model rate constants and concentrations of species are as described in SI Section 1.2, and the rates for toehold occlusion reactions are as given in SI Section 1.3.

In addition to toehold occlusion, it is also important to consider the effects of synthesis errors on the kinetics of DSD reactions. All commercially synthesized strands of DNA have some degree of synthesis errors. As a result the addition of any species introduces a subpopulation of erroneous sequences within the concentration of that species that is added. Even after commercial PAGE or HPLC strand purification, it is typical to have a significant population of strands with erroneous sequences. These impurities generally consist of the deletion of one or more nucleotides, often near the end of the synthesized strand. Most importantly for the operation of the sequential release circuit, these synthesis errors can create subpopulations of DNA complexes with a deletion in the cover strand, resulting in an uncovered toehold domain that is one base longer than it would otherwise be and thus can increase the relevant reaction rate constants by an order of magnitude in this impure population. We were primarily concerned with the fast population of impure Source species, because the clock reaction determines the rate of the entire downstream circuit, which we will model very approximately as a 10% population of Source with an extra nucleotide in the toehold domain. When we include this impure population of Source complex in our Three Step Model without toehold occlusion of the clocked sequential release circuit, we observe faster kinetics of the initial release stages and a more pronounced slowdown of the release rate from one stage to the next as the faster Source population more rapidly depletes (Fig. S11.6). Including both toehold occlusion and the presence of incorrectly synthesized strands in models of the sequential release circuit results in kinetics where there are less discrete release stages (compared to Figure S11.4) in which downstream stages begin to trigger before all upstream outputs are completely released, and where there is a pronounced slowdown in the rate of release from one stage to the next (unclocked Fig. S11.7, clocked Fig. S11.8). Both of these effects are observed in the measured kinetics of the sequential release circuit (Main Text Fig. 4c).

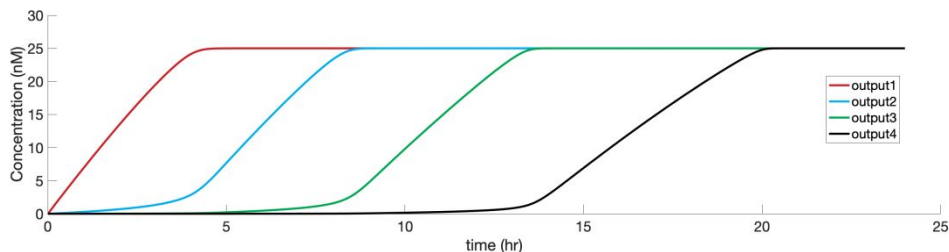


Figure S11.6: Simulated kinetics of the clocked sequential release circuit using the Three Step Model for the DSD reactions (SI Equations XX-YY) and incorporating a subpopulation impure population of Source complex and no toehold occlusion. This simulation used 25 nM Payloads,  $37.5 \cdot (4 - i)$  nM  $\text{Convert}_{i,i+1}$ , for  $i=1$  to 4, and  $1 \mu\text{M}$  of Source and Initiator. The Three Step Model rate constants and concentrations of species are as described in SI Section 1.2.

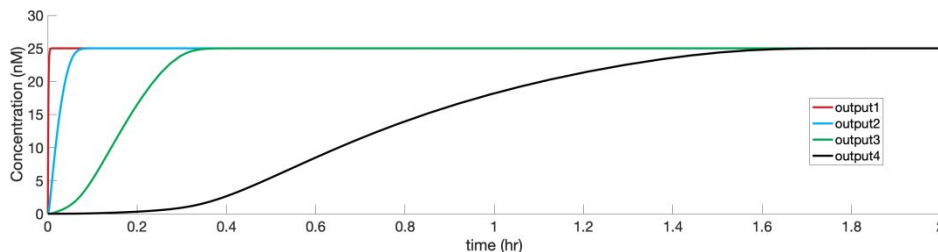


Figure SI1.7 Simulated kinetics of the unlocked sequential release circuit using a Three Step Model for the DSD reaction model (SI Equations XX-XX), including a subpopulation of incorrectly synthesized Source complex (see SI Section 1.3 text) and incorporating toehold occlusion reactions involving the Initiator complex (SI Equation XX). The Three Step Model rate constants and concentrations of species are as described in SI Section 1.2, and the rates for the toehold occlusion reactions are as given in SI Section 1.3.

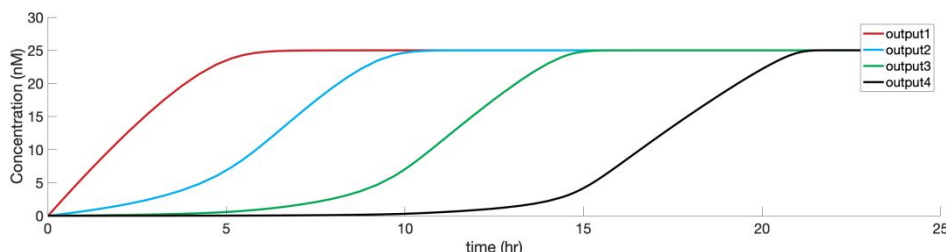


Figure SI1.8: Simulated kinetics of the unlocked sequential release circuit using a Three Step Model for the DSD reaction model (SI Equations XX-XX), including a subpopulation of incorrectly synthesized Source complex (see SI Section 1.3 text) and incorporating toehold occlusion reactions involving the Initiator complex (SI Equation XX). The Three Step Model rate constants and concentrations of species are as described in SI Section 1.2, and the rates for the toehold occlusion reactions are as given in SI Section 1.3.

#### SI1.4 Tuning the Concentration of an Output Released at a Particular Stage

The concentration of Output molecule released at a particular stage of the sequential release circuit is determined by the initial concentration of the corresponding Payload for that stage. In principle, every Payload molecule in the reaction will eventually release its corresponding Output molecules so long as (1) the total concentration of  $\text{Trigger}_1$  (either within the Source or supplied as a single strand as in the unlocked reaction) is greater than the sum of the concentrations of the Payload complexes for all stages, and (2) the concentration of Convert species for each stage is greater than the sum total of all Payload complexes for all downstream stages. The concentrations of the Output released different stages can be different, so long as the concentrations of the Convert species and the  $\text{Trigger}_1$  (or Source and Initiator) are tuned appropriately as described here to allow for complete release. Figure SI1.9 shows, using a simulation of the clocked sequential release circuit, how the circuit can be tuned such that each stage releases a concentration of its corresponding output that is greater than that released in the previous stage.

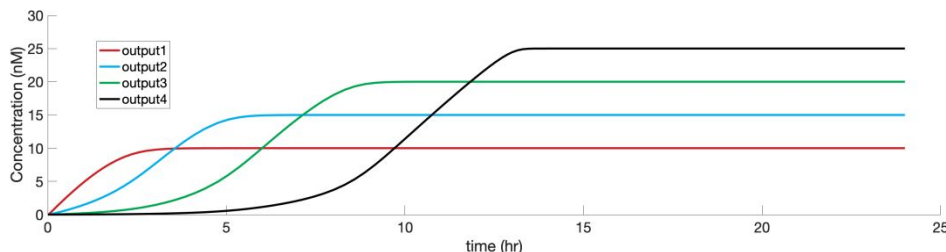


Figure SI1.9: Simulated kinetics of the clocked sequential release circuit using the Three Step Model of DSD reactions and incorporating the effects of an impure population of Source complex and toehold occlusion reactions involving the Initiator complex as described in SI Section 1.4. The concentrations of Payloads for stages 1, 2, 3, and 4 are 10, 15, 20, and 25 nM respectively. The concentrations of Covert species for stages 1, 2, and 3 are 90, 67.6, and 37.5 nM respectively. This simulation used and  $1 \mu\text{M}$  of Source and Initiator. Rate constants for the Three State Model reactions are as given in the text of SI Section 1.2 and the rate constants

for the toehold occlusion reactions and the reactions involving the subpopulation of Source complex are as given in SI Section 1.3.

### SI1.5 Tuning the Timing of Release

In the clocked sequential release circuit, the overall timing of the release process is governed by the effective production rate ( $k_{prod}$ ) of  $Trigger_1$ . The overall speed of the release process can therefore be increased or decreased globally by increasing or decreasing  $k_{prod}$  (Fig. SI1.10). Tuning the time at which one species within the cascade without effecting the timing of all of the other release stages is less straightforward. One potential way to add additional control over the timing of release of specific species would be to incorporate additional dummy delay stages into the cascade, which releases a dummy strand whose sequence is different than the sequences of the other released strands and does not interact with other components of the system or downstream reactions. By adjusting the initial concentrations of a dummy Payload for release stages inserted between existing stages, the start time of the next stage of the cascade after the dummy Payload can be specified independently of the timing of the other Outputs. The timing of all release stages can be specified independently of one another by inserting and tuning the concentrations of dummy Payloads between each pair of release stages (Fig. SI1.11).

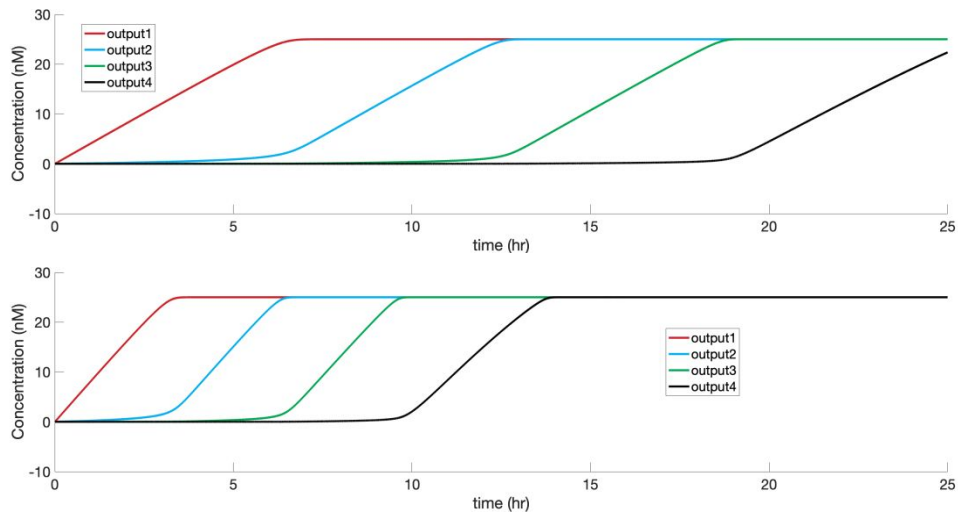


Figure SI1.10: Simulated kinetics of two clocked sequential release circuits using bimolecular model showing how the overall rate of release can be tuned by tuning the clock production rate  $k_{prod}$  for the clock reaction (Main text Eqn. 4). Top: results from a simulation in which  $k_{prod}=100\text{nM/day}$ . Bottom: results from a simulation in which  $k_{prod}=200\text{nM/day}$ . Increasing  $k_{prod}$  increases the overall rates of release. These simulations used 25 nM Payloads and  $37.5 \cdot (4 - i)$  nM  $Convert_{i,i+1}$ , for  $i=1$  to 4 and the bimolecular reactions and rates for reactions given in SI Text 1.1.

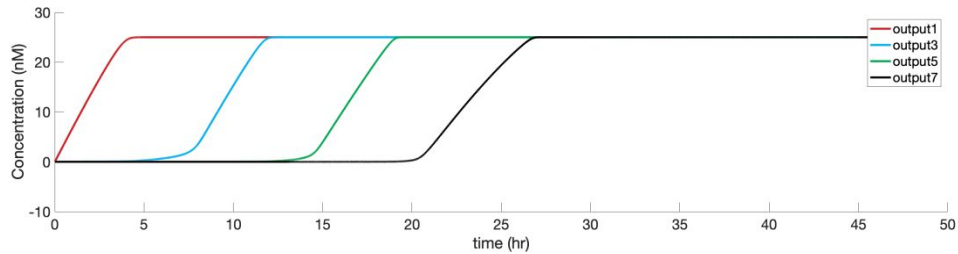


Figure SI1.11 Simulated kinetics of a clocked sequential release circuit with “dummy” delay stages 2, 4 and 6. In this simulation, we used main text Eqn. 4 as the clock reaction with  $k_{prod}=200\text{nM/day}$ . For the Payload species we used 25, 25, 25, 15, 25, 5, and 25 nM for stages 1 through 7 respectively. For the Convert species we used 180, 142.5, 105, 82.5, 45, and 37.5 nM for stages 1 through 7 respectively. The simulation used the bimolecular reactions for the release process and rates for reactions given in SI Text 1.1.

### S11.6 Matlab Simulation Code

Below is the Matlab code used to simulate the above models.

```
clear all %#ok<CLALL>
close all
clc

%INPUT VARIABLES
runTime=24*3600;%The time to run the simulation for (s)
runIdeal=1;
run3SM=1;
cSignal1=0.1125;%uM
cPayload=[0.025,0.025,0.025,0.025];%uM
numStages=4;
convertFactor=1.5;%ratio of [convert] to [payload]
includeClock=1;
cSource=1;%uM
includeOcclusionIn3SM=1*1;
impurityFactorIn3SM=1*0.1;

if runIdeal
    %Ideal CRN calculations
    kPayload=4;%uM^-1 s^-1 (7nt toe)
    kConvert=0.02;%uM^-1 s^-1 (4nt toe)
    kSource=0.2*10^-5;%uM^-1s^-1 (0nt toe)

    %Construct CRN
    crn=simCRN();
    if includeClock

crn.addRxn({'source','initiator'},{'signal1'},kSource,0);%bimolecular
clock
        %crn.addRxn({},{'signal1'},(0.200)/(24*3600),0);%unimolecular
clock
        crn.setConcentration('source',cSource);
        crn.setConcentration('initiator',cSource);
    else
        crn.setConcentration('signal1',cSignal1);
    end
    for i=1:numStages
        %payload

crn.addRxn({'signal',num2str(i)},['payload',num2str(i)]},{'output',nu
m2str(i)}},kPayload,0);
        crn.setConcentration(['payload',num2str(i)],cPayload(i));
        %convert
        if i<numStages%we don't need a convert reaction for the final
stage

crn.addRxn({'signal',num2str(i)},['convert',num2str(i)]},{'signal',nu
m2str(i+1)}},kConvert,0);

        crn.setConcentration(['convert',num2str(i)],convertFactor*sum(cPayload(
i+1:end)));%uM
    end
end
```

```

crn.runSim(runTime,@ode45);

%plots
species2Plot={'output1','output3','output5','output7'};
figure('Position',[10 10 6*300 1.25*300]);
hold on

plotColors={ [203,32,39]/255, [0,174,239]/255, [0,166,81]/255, [0,0,0], [1,0,0] };
for i=1:length(species2Plot)

plot(crn.time/3600,crn.conc(crn.getSpeciesIdsByNames(species2Plot{i}),:)*1000,'LineWidth',3,'Color',plotColors{i});
end
legend(species2Plot);
xlabel('time (hr)');
ylabel('Concentration (nM)');
set(gca, 'FontSize',21);
end

if run3SM
%3SM Calculations
kf=3.5;%uM^-1 s^-1
RT=1.987*10^-3*298;%kcal/mol at room temp
nRec=21;%bases in the recognition domain
kb=400/(nRec^2);%s^-1
ePayload=-9.2;% kcal/mol
eConvert=-4.7;%kcal/mol
e0nt=1.9;%0nt toehold
krConvert=kf*10^6*(2/nRec)*exp(eConvert/RT);
kr0nt=kf*10^6*(2/nRec)*exp(e0nt/RT);
eSource=1.9;
krSource=kf*10^6*(2/nRec)*exp(eSource/RT);
eSourceImpure=0.2;
krSourceImpure=kf*10^6*(2/nRec)*exp(eSourceImpure/RT);
%occlusion
eOccludePayload=-6.9;%kcal/mol
krOccludePayload=kf*10^6*(2/nRec)*exp(eOccludePayload/RT);
eOccludeConvert=-4.7;%kcal/mol
krOccludeConvert=kf*10^6*(2/nRec)*exp(eOccludeConvert/RT);
kbOcclude=400./([9,2,2,2,2,2,2,2,2,2].^2);%s^-1

species2Plot={};
crn2=simCRN();
if includeClock

crn2.addRxn({'source','initiator'},{'sourceInitiator'},2*kf,krSource);%
toehold binding (x2 for initiation on both sides)

crn2.addRxn({'sourceInitiator'},{'initiatorSource'},kb,kb);%branch
migration

crn2.addRxn({'initiatorSource'},{'signal1','sourceWaste'},krSource,kf*2);%dissociation
crn2.setConcentration('source',cSource*(1-impurityFactorIn3SM));

```

```

    crn2.setConcentration('initiator',cSource);
    %impure production

crn2.addRxn({'sourceImpure','initiator'},{'sourceInitiatorImpure'},2*kf
,krSourceImpure);%toehold binding (x2 for initiation on both sides)

crn2.addRxn({'sourceInitiatorImpure'},{'initiatorSourceImpure'},kb, kb);
%branch migration

crn2.addRxn({'initiatorSourceImpure'},{'signal1','sourceWasteImpure'},k
rSource,kf*2);%dissociation

crn2.setConcentration('sourceImpure',cSource*impurityFactorIn3SM);
    else
        crn2.setConcentration('signal1',cSignal1);
    end
    for i=1:numStages
        species2Plot{i}=['output',num2str(i)];
        %payload
        krPayload=kf*10^6*(2/nRec)*exp(ePayload(1)/RT);

crn2.addRxn({'signal',num2str(i)},['payload',num2str(i)]},{'signalPay
load',num2str(i)}},kf,krPayload);%toehold binding

crn2.addRxn({'signalPayload',num2str(i)}},{'outputWaste',num2str(i)}
, kb, kb);%branch migration

crn2.addRxn({'outputWaste',num2str(i)}},{'output',num2str(i)},['waste
',num2str(i)]},kr0nt,kf);%dissociation
        crn2.setConcentration(['payload',num2str(i)],cPayload(i));
        if includeOcclusionIn3SM

crn2.addRxn({'initiator',['payload',num2str(i)]},{'initiatorPayload',n
um2str(i)}},kf,krOccludePayload);%toehold binding

crn2.addRxn({'initiatorPayload',num2str(i)}},{'payloadInitiator',num2
str(i)}},kbOcclude(i),kbOcclude(i));%branch migration
        end
        %convert
        if i<numStages%we don't need a convert reaction for the final
stage

crn2.addRxn({'signal',num2str(i)},['convert',num2str(i)]},{'signalCon
vert',num2str(i)}},kf,krConvert);%toehold binding

crn2.addRxn({'signalConvert',num2str(i)}},{'convertSignal',num2str(i)
}], kb, kb);%branch migration

crn2.addRxn({'convertSignal',num2str(i)}},{'signal',num2str(i+1)},['c
onvertWaste',num2str(i)]},kr0nt,kf);%dissociation

crn2.setConcentration(['convert',num2str(i)],convertFactor*sum(cPayload
(i+1:end)));%uM

        if includeOcclusionIn3SM

crn2.addRxn({'initiator',['convert',num2str(i)]},{'initiatorConvert',n

```

```

um2str(i)]},kf,krOccludeConvert);%toehold binding

crn2.addRxn({'initiatorConvert',num2str(i)}},{['convertInitiator',num2
str(i)]},kbOcclude(i),kbOcclude(i));%branch migration
    end
end
end
crn2.runSim(runTime,@ode15s);

%plots
figure('Position',[10 10 6*300 1.25*300]);
hold on

plotColors={ [203,32,39]/255,[0,174,239]/255,[0,166,81]/255,[0,0,0],[1,0
,0]};
    for i=1:length(species2Plot)

plot(crn2.time/3600,crn2.conc(crn2.getSpeciesIdsByNames(species2Plot{i}
),:)*1000,'LineWidth',3,'Color',plotColors{i});
    end
    legend(species2Plot);
    xlabel('time (hr)');
    ylabel('Concentration (nM)');
    set(gca,'FontSize',21);
end

```

### SI2: Eliminating sequence overlap between output strands

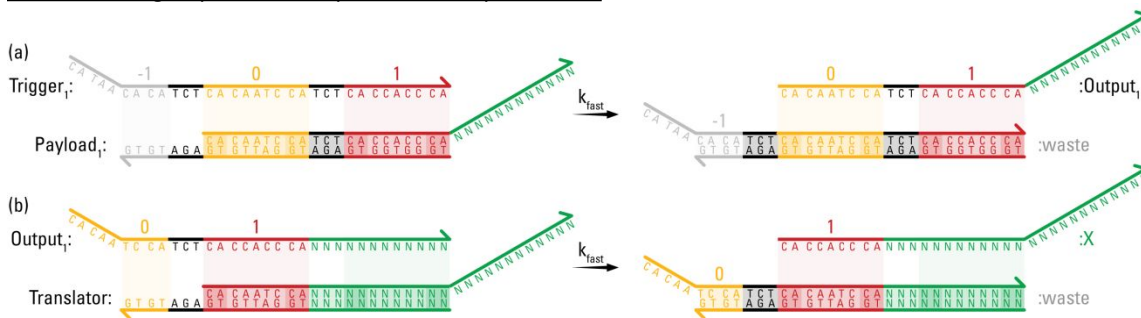


**Figure SI2.1:** A DNA strand displacement (DSD) translator reaction that could be used to decouple the sequences of the Output strands from the rest of the sequential release circuit. Arbitrary bases are indicated by an “N”. (a) In the sequential release circuit, Trigger<sub>1</sub> releases Output<sub>1</sub> from Payload<sub>1</sub>. This is the same reaction as presented in Figure 2a, except the quencher-fluorophore pair has been replaced by an overhanging sequence. (b) Output<sub>1</sub> next binds to the Translator complex, displacing species X, which contains an arbitrary sequence (green) that is independent from Trigger<sub>1</sub>. These new domains could be used to interact independently with downstream systems. Note that depending on the application, there are multiple different ways to design such a translator reaction.

### SI3: Methods

All DNA strands were obtained from Integrated DNA Technologies (IDT), using the purification options listed in SI Table 1. On arrival all strands were suspended in Millipore purified water at a concentration of about 1mM and stored at -20°C. Stock concentrations were determined by measuring the absorbance of light at a wavelength of 260nm (OD260), together with the extinction coefficient for each strand provided by IDT (EXT), using the Beer-Lambert law: [ssDNA]=OD260/EXT.

We prepared each of the double-stranded complexes (Source, Payloads, Converts and iConverts) separately at 100 μM in Tris-acetate-EDTA buffer with 12.5 mM Mg<sup>++</sup> (1x TAE/Mg<sup>++</sup>). The Source, Payload, and Convert complexes were prepared with a 1.2x excess of their respective top strands (*i.e.* 120 μM of either Trigger, or Output strand) to ensure all bottom strands were occupied by a top strand. The iConvert complexes were prepared with a 1.2x excess of both of their top strands (*i.e.*, the Trigger and Protect strands). We then annealed all complexes in an Eppendorf Mastercycler PCR, first heating the solutions to 90°C, holding the temperature constant for 5 minutes, and then cooling at -0.1°C per every 6 seconds down to 20°C. The Source, Convert, and iConvert complexes were purified by polyacrylamide gel electrophoresis (PAGE). Payload complexes were not gel purified.

For gel purification, we cast 15% polyacrylamide gels by mixing 3.25mL of 19:1 40% acrylamide/bis solution (Bio-Rad) with 1.3mL 10x TAE/Mg<sup>++</sup> and 8.45mL Millipore-purified H<sub>2</sub>O, and initiated polymerization with 75μL 10% ammonium persulfate (APS, Sigma Aldrich) and 7.5μL tetramethylethylenediamine (TEMED, Sigma Aldrich). We mixed 200 μL of dsDNA complex with 6x loading dye (New England Biolabs, product #B7021S) and loaded into a Scie Plas TV100K cooled vertical electrophoresis chamber. We ran our gels at 150V and 4°C for 3 hours and then cut out the purified bands using UV-shadowing at 254nm<sup>SI-R3</sup>. The gel bands were chopped into small pieces, mixed with 300μL of 1x TAE/Mg<sup>++</sup> buffer, and then left on a lab bench overnight to allow the DNA to diffuse out of the gel into the buffer. The next day, the buffer was transferred by pipet to a fresh tube, leaving behind as much of the gel as possible. These fresh tubes were centrifuged for 5 minutes to draw any remaining gel pieces to the bottom of the tube, and then transferred to yet another fresh tube, leaving behind ~50μL of gel/solution at the bottom. The concentrations of these purified complexes were then measured with an Eppendorf Biophotometer, using the approximate extinction coefficient  $EXT = EXT_{top\_strand} + EXT_{bottom\_strand} - 3200N_{AT} - 2000N_{GC}$ , where  $N_{AT}$  and  $N_{GC}$  are the number of hybridized A-T and G-C pairs in each complex, respectively.<sup>SI-R4</sup> All resulting complexes were stored at 4°C.

Reaction kinetics were measured on quantitative PCR (qPCR) machines (Agilent Stratagene Mx3000 and Mx3005 series) at 25°C. Fluorescence was typically measured every 30 seconds for baseline measurements and for the first 1-2 hours after a reaction was triggered by adding Trigger<sub>1</sub> or Initiator, to accurately capture the early kinetics of a reaction, and then every 5 minutes for the remainder of the experiment to avoid photobleaching the fluorophores. Reactions were prepared in 96-well plates using 50μL/well volume. Each well

contained 1x TAE/Mg<sup>++</sup> and 1  $\mu$ M of 20-mer PolyT strands to help displace reactant species from the pipet tips used to add them to the well. In a typical experiment, Millipore-purified H<sub>2</sub>O, TAE/Mg<sup>++</sup> and PolyT<sub>20</sub> strands were first mixed together. All necessary Payload complexes were then added and a measurement of the baseline reporter fluorescence was taken to determine what fluorescence corresponded to the state of the system with zero output signal. We then add any other DNA reactant species, in the amounts specified for each experiment, and tracked the resulting kinetics. Data was processed according to the steps in SI5.

#### SI4: Sequences

The sequences of our domains were drawn from Table S1 of the Supporting Online Material for reference SI-R3. We used NuPack<sup>SI-R5</sup> to verify that the secondary structures of our strands and complexes matched the designed structures presented in the main text. Sequences for each strand used in the study are listed in SI Table 1. The complexes referred to in the main text as Payload 2 and Payload 2A are identical. The codes /5HEX/, /56-FAM/, /5TexRd-XN/, /5Cy5/, stand for the fluorophores we used (HEX, FAM, Texas Red, and Cy5 respectively), while the codes /3IABkFQ/ and /3IABRQSp/ stand for the Iowa Black quencher modifications we used to quench our fluorophores.

**SI Table 1: Sequence Data**

Strand	Sequences	IDT Purification
Trigger 1	CA TAACA CA TCT CA CAATC CA TCT CA CCACC CA	PAGE
Source Bottom	TG GATTG TG AGA TG TGTTA TG	PAGE
Initiator	CA TAACA CA TCT CA CAATC CA	PAGE
Payload 1 Top	CA CAATC CA TCT CA CCACC CA/3IABkFQ/	HPLC
Payload 1 Bottom	/5HEX/TG GGTGG TG AGA TG GATTG TG AGA TG TG	HPLC
Convert 1,2 Bottom	TG GGTGG TG AGA TG GATTG TG AGA T	PAGE
Trigger 2	CA CAATC CA TCT CA CCACC CA TCT CA AAAC T CA	PAGE
Payload 2 Top	CA CCACC CA TCT CA AAAC T CA/3IABkFQ/	HPLC
Payload 2 Bottom	/56-FAM/TG AGTTT TG AGA TG GGTGG TG AGA TG GA	HPLC
Convert 2,3 Bottom	TG AGTTT TG AGA TG GGTGG TG AGA T	PAGE
Trigger 3	CA CCACC CA TCT CA AAAC T CA TCT CA TCCAA CA	PAGE
Payload 3 Top	CA AAAC T CA TCT CA TCCAA CA/3IABRQSp/	HPLC
Payload 3 Bottom	/5TexRd-XN/TG TTGGA TG AGA TG AGTTT TG AGA TG GG	HPLC

<b>Convert 3,4 Bottom</b>	TG TTGGA TG AGA TG AGTTT TG AGA T	PAGE
<b>Trigger 4</b>	CA AAAC T CA TCT CA TCCAA CA TCT CA TCAAT CA	PAGE
<b>Payload 4 Top</b>	CA TCCAA CA TCT CA TCAAT CA/3IABRQSp/	HPLC
<b>Payload 4 Bottom</b>	/5Cy5/TG ATTGA TG AGA TG TTGGA TG AGA TG AG	HPLC
<b>Deprotect 1,2A</b>	CCTAC CTTCACTACTA	PAGE
<b>iConvert 1,2A Bottom</b>	TG GGTGG TG AGA TG GATTG TG AGA T TAGTTGTGAAG GTAGG	PAGE
<b>Protect 1,2A</b>	CTTCACTACTA ATCT	PAGE
<b>Deprotect 1,2B</b>	CCTAC TATCTAATCTC	PAGE
<b>iConvert 1,2B Bottom</b>	TG GGTGG TG AGA TG GATTG TG AGA T GAGATTAGATA GTAGG	PAGE
<b>Protect 1,2B</b>	TATCTAATCTC ATCT	PAGE
<b>Payload 2B Top</b>	CA CCACC CA TCT CA TCCAA CA/3IABRQSp/	HPLC
<b>Payload 2B Bottom</b>	/5TexRd-XN/TG TTGGA TG AGA TG GGTGG TG AGA TG GA	HPLC

### SI5: Reporter Calibrations

For main text Fig. 3 and Fig. 4c, the presented data was normalized by first adding all of the necessary Payload species, and then measuring the baseline fluorescence corresponding to no Trigger species added, for 10 minutes sampling every 30 seconds. For each fluorescence channel, this baseline fluorescence was then averaged and subtracted from the rest of the data set. Finally, each fluorescence channel was then divided by the maximum fluorescence counts detected in the experiment for that channel. The same normalization process was used to process the data in Fig. 5, except the FAM and TEX fluorescence data was divided by the maximum fluorescence detected in *both* Fig. 5c and 5d for those channels, rather than treating these plots independently.

Concentrations of  $\text{Trigger}_1$  reported in the main text Figure 4b were determined by comparing the change in fluorescence to a set of empirical calibration curves determined as follows. Known concentrations of  $\text{Trigger}_1$  were added to a solution containing 300 nM of  $\text{Payload}_1$  (Fig. SI5.1).  $\text{Trigger}_1$  reacts irreversibly with  $\text{Payload}_1$  to separate a quencher-fluorophore pair, increasing fluorescence. For each trajectory, we then calculate a calibration coefficient  $\alpha$  that relates the increase in fluorescence to the concentration of  $\text{Trigger}_1$  added:

$$\alpha \equiv \frac{[\text{Trigger}_1]}{\Delta \text{RawCPS}}$$

$\Delta \text{RawCPS}$  is the difference between the fluorescence intensity the end of the experiment and the fluorescence intensity before the  $\text{Trigger}_1$  strand is added. We took the average  $\bar{\alpha}$  for all of the different

calibration trajectories. We then use this factor to calculate the concentration of  $\text{Trigger}_1$  released in the experiments shown in Figure 4b as follows:

$$[\text{Trigger}_1](t) \equiv \bar{\alpha} \cdot \Delta\text{RawCPS}(t)$$

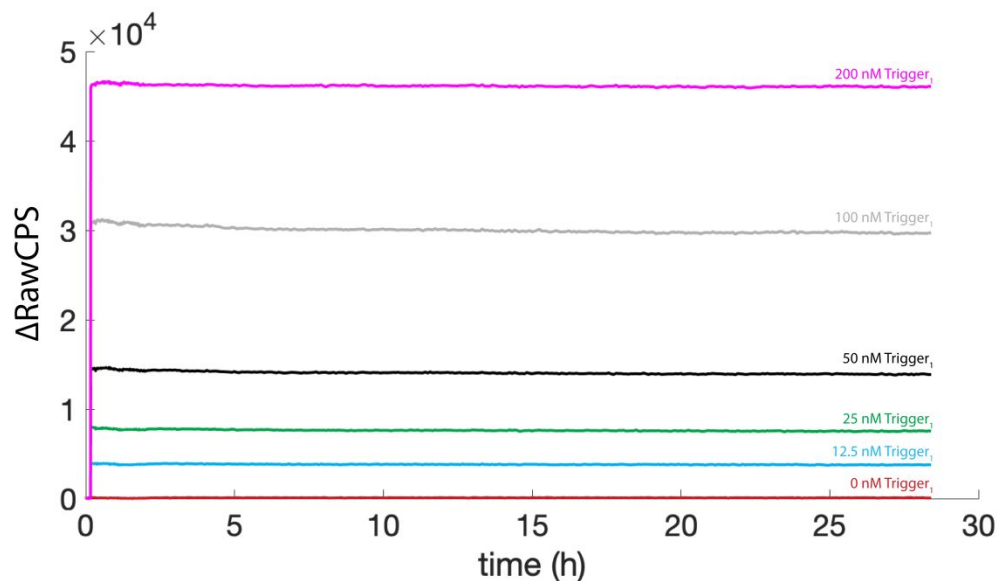


**Figure S15.1:** Calibration curves to convert from raw fluorescence in counts per second to the concentration of  $\text{Trigger}_1$  in Figure 4b.

*S16: Untriggered cascade, negative control*

To test that the sequential release cascade does not substantially release its outputs unless  $\text{Trigger}_1$  is added, we prepared a solution containing 25 nM of each of the four Payloads, along with 112.5 nM of  $\text{Convert}_{1,2}$ , 75 nM of  $\text{Convert}_{2,3}$ , and 37.5 nM of  $\text{Convert}_{3,4}$ , and triggered it by adding 100 nM of all four  $\text{Trigger}$  strands after approximately 20 hours (Fig. S16.1). For this particular experiment, the  $\text{Convert}$  species were annealed with a 1.1:1 ratio of top strand to bottom strand, and were not gel purified after annealing. The resulting fluorescence data was normalized by subtracting the minimum fluorescence value from each trajectory, and dividing each trajectory by the maximum fluorescence value.

We observed no significant untriggered leak fluorescence for the HEX and FAM channels (corresponding to Payloads 1 and 2), but we did observe nonzero fluorescence corresponding to approximately 15% of the maximum signal for the TEX and Cy5 channels (corresponding to Payloads 3 and 4).

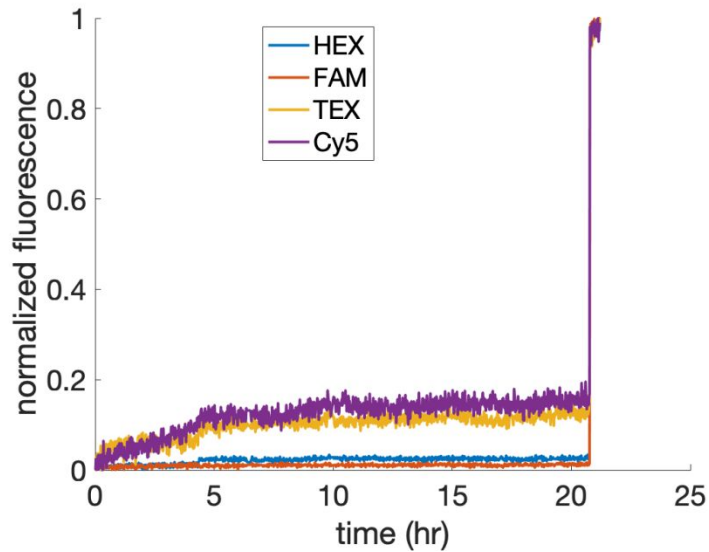


**Figure SI6.1:** An unlocked sequential release cascade with no trigger molecules added until the end of the experiment.

### SI7. Supplemental References

- [SI-R1] Zhang, David Yu, and Erik Winfree. "Control of DNA strand displacement kinetics using toehold exchange." *J. Am. Chem. Soc.* 131.47 (2009): 17303-17314.
- [SI-R2] Scalise, Dominic, Nisita Dutta, and Rebecca Schulman. "DNA strand buffers." *J. Am. Chem. Soc.* 140.38 (2018): 12069-12076.
- [SI-R3] Qian, L.; Winfree, E. "Scaling up digital circuit computation with DNA strand displacement cascades." *Science* 2011, 332.6034, 1196-1201.
- [SI-R4] Seelig, G.; Soloveichik, D.; Zhang, D. Y.; Winfree, E. (2006) Enzyme-free nucleic acid logic circuits. *Science*, 314.5805, 1585-1588.
- [SI-R5] J. N. Zadeh, C. D. Steenberg, J. S. Bois, B. R. Wolfe, M. B. Pierce, A. R. Khan, R. M. Dirks, N. A. Pierce. NUPACK: analysis and design of nucleic acid systems. *J Comput. Chem.*, 32:170–173, 2011.